

## Multifunctional Chemical Vapor Sensors of Aligned Carbon Nanotube and Polymer Composites

Chen Wei,<sup>†</sup> Liming Dai,<sup>\*,†</sup> Ajit Roy,<sup>‡</sup> and Tia Benson Tolle<sup>‡</sup>

Department of Chemical and Materials Engineering, School of Engineering, University of Dayton, Dayton, Ohio 45469-0240, and Air Force Research Laboratory, Materials and Manufacturing Directorate, MLBC, Wright-Patterson AFB, Ohio 45433-7750

Received October 16, 2005; E-mail: ldai@udayton.edu

With the recent developments in nanoscience and nanotechnology, there is a pressing need for flexible, mechanically robust, and environmentally stable chemical vapor sensors with a high efficiency and low power consumption. This type of sensors can, for example, be used for real-time sensing of chemical warfare stimulants in a battlefield by monitoring the resistance changes in soldiers' clothing.<sup>1</sup> The early measurements on the conductivity changes of conjugated (conducting) polymers via charge transfer with certain chemical vapors or nonconducting polymers mixed with conductive fillers through polymer swelling by gas absorption around the percolation threshold provided the basis for developing polymer-based chemical vapor sensors.<sup>1–3</sup> However, the poor environmental stability associated with most conjugated polymers limited the scope of their use for practical applications.<sup>1</sup> The uncertainty on the precise location of the percolation threshold in random dispersion systems remained as one of the major hindrances toward high-performance conductively filled polymer sensors.<sup>1–3</sup>

The recent discovery of the gas sensing capabilities of carbon nanotubes through the charge transfer or capacitance change by gas absorption (e.g., NH<sub>3</sub>, NO<sub>2</sub>, O<sub>2</sub>)<sup>4–6</sup> is significantly intriguing as their small size, high surface area, good environmental stability, and excellent mechanical and electronic properties can offer many advantages for sensing applications.<sup>1,7</sup> The use of the pristine *non-aligned* carbon nanotubes for gas sensing as reported in these studies often involves tedious processes for integrating single carbon nanotubes into sensor devices, and the number of analytes to be determined is also hampered by the limited specific interactions with the unmodified nanotubes. It will be a significant advancement if we can use *perpendicularly aligned* carbon nanotube arrays as the sensing materials. Aligned carbon nanotube arrays, in either a patterned or nonpatterned form,<sup>8</sup> allow the development of novel sensors and/or sensor chips without the need for direct manipulation of individual nanotubes since the constituent nanotubes can be *collectively* addressed through a common substrate/electrode.<sup>8,9</sup> The aligned nanotube structure further provides a large well-defined surface area and the capacity for modifying the carbon nanotube surface with various transduction materials<sup>8,9</sup> to effectively enhance the sensitivity and to broaden the scope of analytes to be detected. Here, we report a novel concept for developing a new class of multifunctional chemical vapor sensors with a low power consumption, high sensitivity, good selectivity, and excellent environmental stability by partially coating *perpendicularly aligned* carbon nanotube arrays with appropriate flexible polymer films.

As schematically shown in Figure 1, the aligned multiwall carbon nanotubes produced by pyrolysis of iron(II) phthalocyanine (Figure 1a)<sup>8,10</sup> were partially covered with a polymer coating top-down along their tube length (Figure 1a (I)) by depositing a droplet of polymer solution (e.g., poly(vinyl acetate), PVAc, polyisoprene,

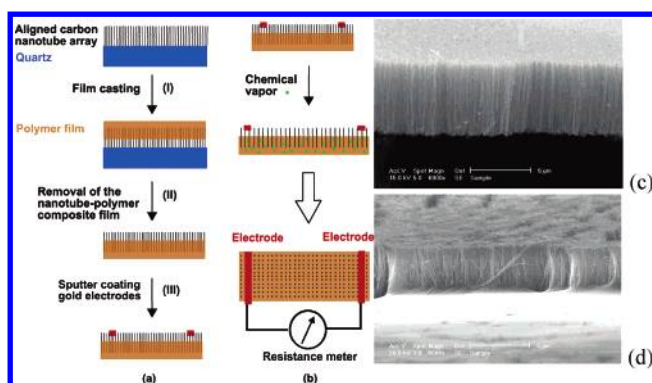


**Figure 1.** Schematic illustration of the procedures for (a) fabricating and (b) characterizing the aligned carbon nanotube–polymer composite chemical vapor sensor. SEM images of the aligned carbon nanotube array (c) before and (d) after being partially coated with a polymer (PVAc) film on top and turned upside down (cf. Supporting Information; scale bars = 5  $\mu\text{m}$ ).

PI) onto the nanotube film (cf. Supporting Information). The composite film was then inverted as a free-standing film (Figure 1a (II)) for sputter-coating two strip electrodes of gold across the nanotube arrays that were protruding from the polymer matrix (Figure 1a (III)). The flexible thin film device can then be used for chemical vapor sensing through monitoring conductivity changes (Figure 1b) caused by the charge-transfer interaction with gas molecules (*without the need for direct manipulation of individual nanotubes*) and/or the inter-tube distance change induced by polymer swelling via gas absorption (*without the requirement to be operated around the percolation threshold*). SEM images c and d of Figure 1 show the aligned carbon nanotube array before and after being partially filled with PVAc, respectively.

As seen in Figure 2a, the *as-synthesized* aligned carbon nanotube arrays without the polymer coating do not show any obvious resistance change while exposed to various chemical vapors, nor does the pure polymer film. In contrast, Figure 2b clearly shows  $\sim 130\%$  increase in the resistance change,  $\Delta R$ , for a composite film of PVAc and aligned carbon nanotubes after being exposed to tetrahydrofuran (THF) vapor for several minutes. Subsequent removal of the THF vapor source caused a loss of ca. 100% in the resistance change after keeping the nanotube–PVAc composite film in air at room temperature for 2 min. It is apparent that the observed resistance changes are due to expansion of the polymer matrix upon exposure to the chemical vapor, which leads to a concomitant increase in the inter-tube distance (Figure 1b). The lost conductivity could not be completely compensated in this particular case, even after drying the nanotube–PVAc composite film in air for a prolonged period, due to the inevitable presence of some residual good solvent (i.e., THF) in the PVAc matrix. After the first vapor–air cycle with a 2 min interval, the maximum resistance and the peak height became constant (Figure 2b), indicating that the solvent absorption/desorption had reached an equilibrium state.

<sup>†</sup> University of Dayton.

<sup>‡</sup> Wright-Patterson AFB.

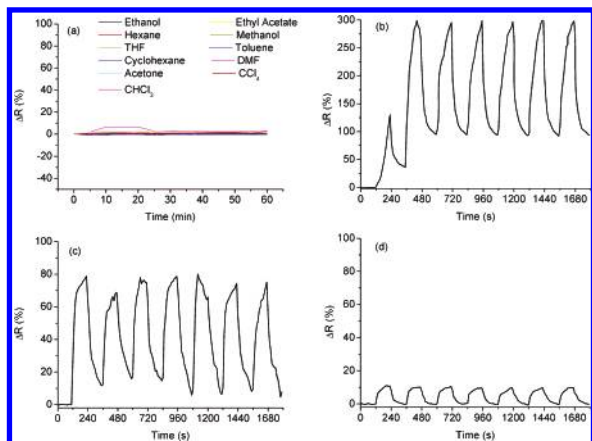


**Figure 2.** Relative variations of the resistance,  $\Delta R$ , for (a) a pure aligned multiwall carbon nanotube array on quartz upon exposure to various chemical vapors, and an aligned carbon nanotube–PVAc film during (b) THF–air cycles, (c) ethanol–air cycles, and (d) cyclohexane–air cycles with time intervals for 2 min “on” and 2 min “off”.  $\Delta R = (R_{\text{vapor}} - R_0)/R_0 \times 100\%$ , where  $R_0$  and  $R_{\text{vapor}}$  are the resistances of the aligned carbon nanotube–polymer composite film before and after exposure to a chemical vapor, respectively.

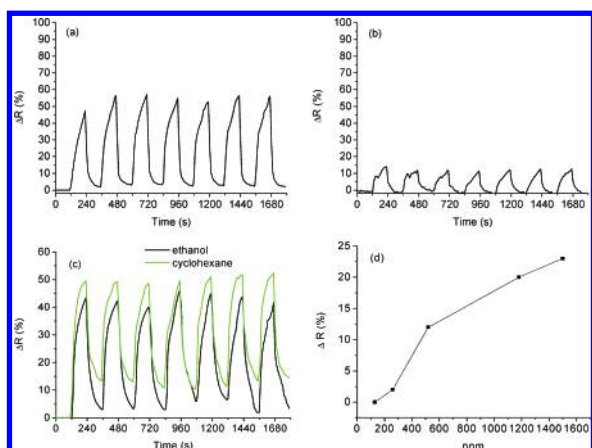


**Figure 3.**  $\Delta R$  for an aligned carbon nanotube–PI film during (a) cyclohexane–air cycles and (b) ethanol–air cycles, and an aligned carbon nanotube–PVAc/PI film during (c) cyclohexane–air and ethanol–air cycles, and (d) its equilibrium resistance peak height versus the partial cyclohexane vapor pressure (cf. Supporting Information).

Similar resistance changes were observed for the aligned carbon nanotube–PVAc composite film when exposed to other chemical vapors (e.g., ethanol, cyclohexane; c and d in Figure 2, respectively). However, the equilibrium peak height for THF is about 290% (Figure 2b), with respect to the corresponding value of ca. 80% for ethanol (Figure 2c). This difference can be attributed to the fact that THF is a better solvent than ethanol and can cause a greater expansion of the PVAc matrix, resulting in a larger change in resistance. The equilibrium peak height could only reach approximately 12% upon exposure to a nonsolvent (e.g., cyclohexane, Figure 2d). Unlike the case with THF, however, the conductivity loss by cyclohexane exposure could be fully recovered within minutes after removal of the vapor source.

By simply replacing PVAc with PI, the weak response of cyclohexane to the aligned carbon nanotube–PVAc composite film sensor was significantly enhanced from a peak height of approximately 12% (Figure 2d) to 55% (Figure 3a). This is attributed to the good solvent ability of cyclohexane for PI. In contrast, ethanol, a poor solvent to PI, only gave weak responses with a peak height of approximately 10% (Figure 3b). Consequently, the composite sensor based on the aligned carbon nanotubes and single component polymer has certain limitations for detecting nonsolvent vapors.

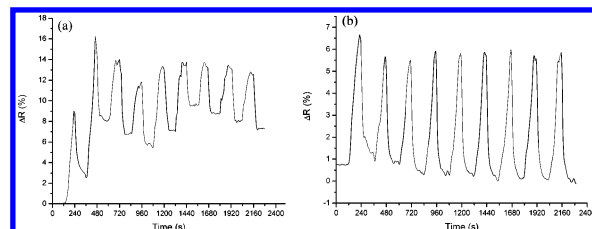


**Figure 4.**  $\Delta R$  for an aligned carbon nanotube–PVAc/PI film with the on/off switching cycles (a) between 20 and 70 °C and (b) under an electric light bulb (cf. Supporting Information).

To broaden the scope of analytes to be detected by an aligned carbon nanotube–polymer composite film sensor, we partially coated the aligned nanotubes (Figure 1a) with a mixture solution of PVAc and PI (weight ratio 50:50) in toluene (2 wt %). As seen in Figure 3c, the chemical vapor sensors based on the aligned carbon nanotubes and PVAc/PI binary polymer composite show reasonably good responses to both cyclohexane (about 50 versus 12% for its pure PVAc counterpart) and ethanol (about 45 versus 10% for its pure PI counterpart). The large-range good correlation between the equilibrium peak height and the partial cyclohexane vapor pressure shown in Figure 3d indicates a high sensitivity and reliability, though the choice of the polymer–vapor pair and device design has not been optimized in this study. The virtually unlimited number of combinations of aligned carbon nanotubes with different polymer systems should make the methodology reported here highly versatile for developing various novel nanotube and polymer sensors for effectively detecting a large variety of chemical vapors (cf. Table S1).

Our preliminary results indicated that these rationally designed, aligned carbon nanotube–polymer composite films are also useful for other applications involving possible film distortions caused, for example, by mechanical, thermal, and/or optical effect(s). The similar resistance changes induced by thermal (Figure 4a) and optical (Figure 4b) exposure cycles as those induced by certain chemical vapor–air cycles clearly indicate that the composite film can also be used for thermal and optical sensing due to the thermal swelling of the polymer substrate caused by either temperature changes or optical absorption (cf. Supporting Information for experimental details and the mechanical deformation sensing (Figure S3)). Therefore, the present study should have important implications for potential use of aligned carbon nanotubes and polymer composites as a new class of very promising multifunctional materials and devices, which could lead to many new applications of carbon nanotubes.

**Acknowledgment.** L.D. thanks the ACS (PRF 39060-AC5M), NSF (CCF-0403130), AFRL/ML-HBCU, WBI, The Dayton Development Coalition, and University of Dayton for financial support.

**Supporting Information Available:** Detailed experimental procedures and results from mechanical deformation sensing. This material is available free of charge via the Internet at <http://pubs.acs.org>.

## References

- (1) Dai, L. *Intelligent Macromolecules for Smart Devices: From Materials Synthesis to Device Applications*; Springer-Verlag: New York, 2004.
- (2) Chen, S. G.; Hu, J. W.; Zhang, M. Q.; Rong, M. Z. *Sens. Actuators B* **2005**, *105*, 187 and references cited therein.
- (3) Koul, S.; Chandra, R.; Dhawan, S. K. *Sens. Actuators B* **2001**, *75*, 151 and references cited therein.
- (4) Kong, J.; Franklin, N. R.; Zhou, C.; Chapline, M. G.; Peng, S.; Cho, K.; Dai, H. J. *Science* **2000**, *287*, 622.
- (5) Collins, G.; Bradley, K.; Ishigami, M.; Zettl, A. *Science* **2000**, *286*, 1801.
- (6) Snow, E. S.; Perkins, F. K.; Houser, S. C.; Badescu, S. C.; Reinecke, T. L. *Science* **2005**, *307*, 1942.
- (7) (a) Meyyappan, M. *Carbon Nanotubes: Science and Applications*; CRC Press: Boca Raton, FL, 2005. (b) Li, J.; Lu, Y.; Ye, Q.; Delzeit, L.; Meyyappan, M. *Electrochem. Solid-State Lett.* **2005**, *8*, H100.
- (8) Dai, L.; Patil, A.; Gong, X.; Guo, Z.; Liu, L.; Liu, Y.; Zhu, D. *ChemPhysChem* **2003**, *4*, 1150 and references cited therein.
- (9) He, P.; Dai, L. *Chem. Commun.* **2004**, 348 and references cited therein.
- (10) Yang, Y.; Huang, S.; He, H.; Mau, A. W. H.; Dai, L. *J. Am. Chem. Soc.* **1999**, *121*, 10832. JA0570335